Production and characterisation of a novel actinobacterial DyP-type peroxidase and its application in coupling of phenolic monomers

Amos Musengi[1,2], Kim Durrell[1], Alaric Prins[1,3], Nuraan Khan[1], Mayowa Agunbiade[1], Tukayi Kudanga[1,4], Bronwyn Kirby-McCullough[3], Brett I. Pletschke[5], Stephanie G. Burton[6], Marilize Le Roes-Hill[1]*

[1]Applied Microbiology and Health Biotechnology Institute, Cape Peninsula University of Technology, PO Box 1906, Bellville, 7535, South Africa
[2]Biotechnology Department, Harare Institute of Technology, P. O. Box BE 277, Belvedere, Harare Zimbabwe
[3]Institute for Microbial Biotechnology and Metagenomics, Department of Biotechnology, University of the Western Cape, Bellville, 7535, South Africa
[4]Department of Biotechnology and Food Technology, Durban University of Technology, PO Box 1334, Durban, 4000, South Africa
[5]Department of Biochemistry and Microbiology, Rhodes University, PO Box 94, Makhanda (Grahamstown), 6140, South Africa
[6]Vice-Principal: Research and Postgraduate Education and Department of Biochemistry, University of Pretoria, Private Bag X20, Hatfield, Pretoria, 0028, South Africa

*Corresponding author: Dr Marilize Le Roes-Hill
E-mail: leroesm@cput.ac.za
Telephone: +27 21 953 8499

Graphical Abstract

Peroxidase purification

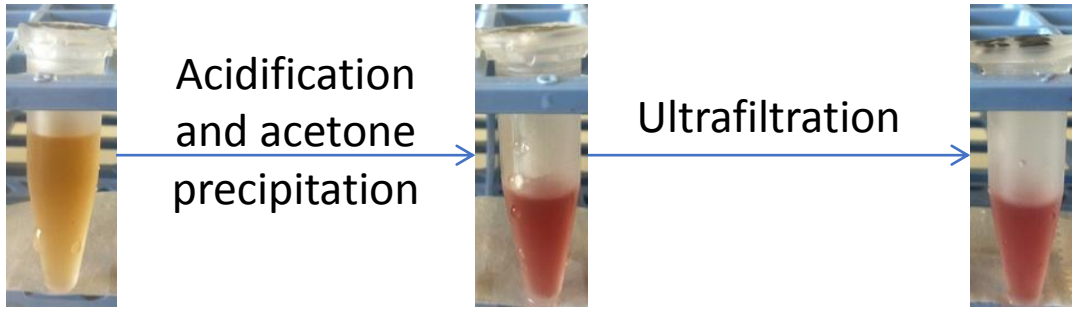

Genomics

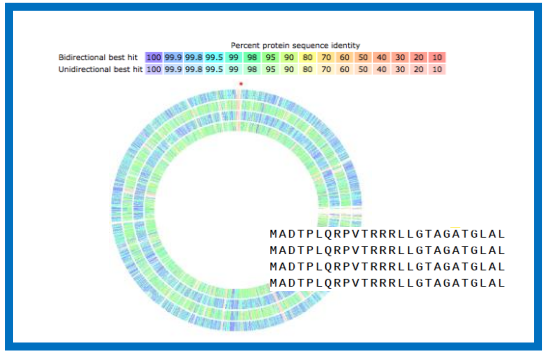

Biochemical characterization

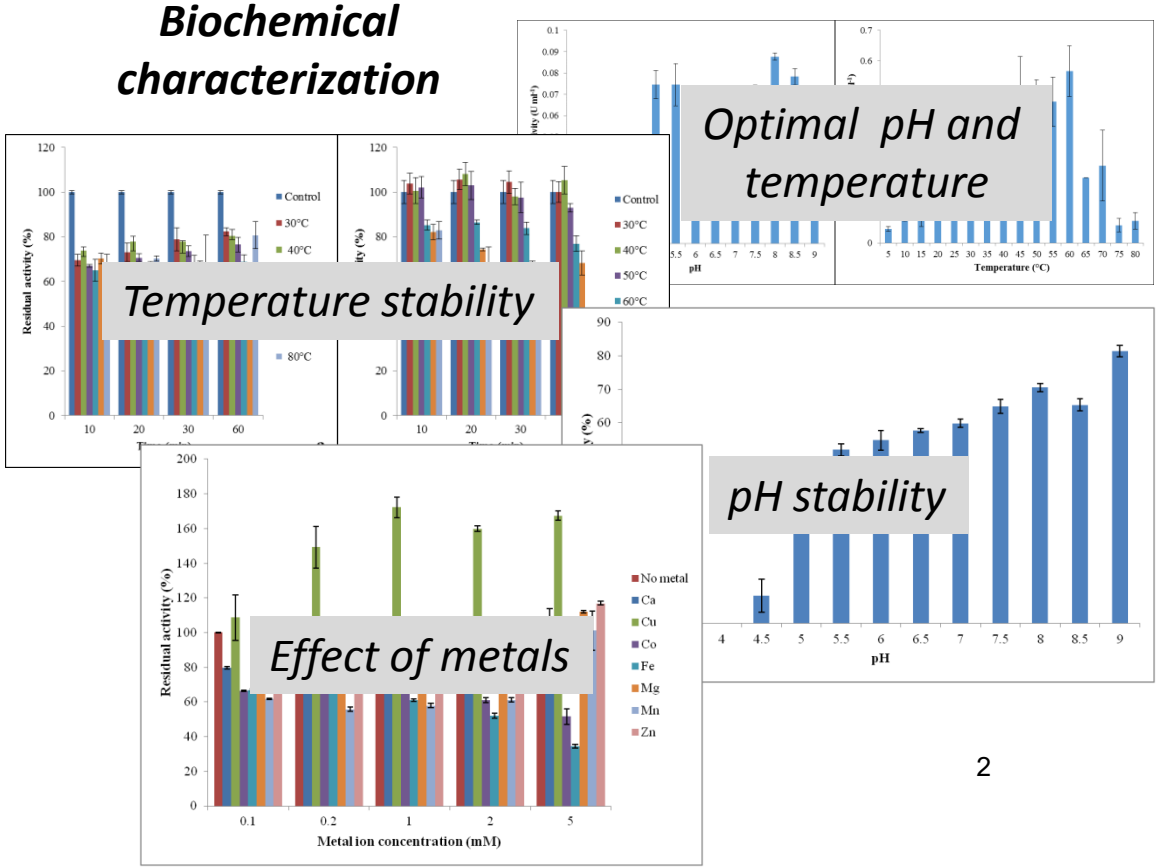

Biocatalysis: Coupling reactions

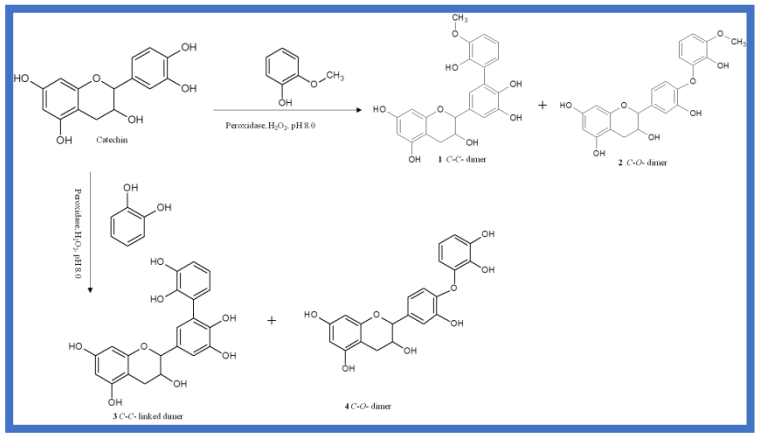

Highlights

- Novel DyP-type peroxidase was produced from native streptomycete strain
- Genome mining and functional studies allowed for identification of the peroxidase
- Stepwise purification process was developed to obtain the purified enzyme
- Biocatalytic application in the coupling of phenolic monomers

Abstract

The extracellular peroxidase from *Streptomyces albidoflavus* BSII#1 was purified to near homogeneity using sequential steps of acid and acetone precipitation, followed by ultrafiltration. The purified peroxidase was characterised and tested for the ability to catalyse coupling reactions between selected phenolic monomer pairs. A 46-fold purification of the peroxidase was achieved, and it was shown to be a 46 kDa haem peroxidase. Unlike other actinobacteria-derived peroxidases, it was only inhibited (27% inhibition) by relatively high concentrations of sodium azide (5 mM) and was capable of oxidising eleven (2,4-dichlorophenol, 2,6-dimethoxyphenol, 4-*tert*-butylcatechol, ABTS, caffeic acid, catechol, guaiacol, L-DOPA, o-aminophenol, phenol, pyrogallol) of the seventeen substrates tested. The peroxidase remained stable at temperatures of up to 80°C for 60 min and retained >50% activity after 24 hours between pH 5.0 – 9.0, but was most sensitive to incubation with hydrogen peroxide (H_2O_2; 0.01 mM), L-cysteine (0.02 mM) and ascorbate (0.05 mM) for one hour. It was significantly inhibited by all organic solvents tested ($p \leq 0.05$). The K_m and V_{max} values of the partially purified peroxidase with the substrate 2,4-DCP were 0.95 mM and 0.12 mmol min^{-1}, respectively. The dyes reactive blue 4, reactive black 5, and Azure B, were all decolourised to a certain extent: approximately 30% decolourisation was observed after 24 h (1 μM dye). The peroxidase successfully catalysed coupling reactions between several phenolic monomer pairs including catechin-caffeic acid, catechin-catechol, catechin-guaiacol and guaiacol-syringaldazine under the non-optimised conditions used in this study. Genome sequencing confirmed the identity of strain BSII#1 as a *S. albidoflavus* strain. In addition, the genome sequence revealed the presence of one peroxidase gene that includes the twin arginine translocation signal sequence of extracellular proteins. Functional studies confirmed that the peroxidase produced by *S. albidoflavus* BSII#1 is part of the dye-decolourising peroxidase (DyP-type) family.

Keywords:

Actinobacteria; biocatalysis; DyP-type peroxidase; purification; *Streptomyces albidoflavus*; genome

Introduction

Peroxidases represent an important class of oxidoreductase enzymes that is characterised by the oxidation of organic and inorganic substrates using, primarily, hydrogen peroxide (H_2O_2) as the electron acceptor. Different types of peroxidases occur in nature and their functions are diverse. Peroxidases derived mainly from plant and fungal sources have been exploited in a number of biotechnological processes that include decolourisation of synthetic dyes [1,2], bioremediation of phenolic and related compounds [3-6], and cell encapsulation [7-10]. Furthermore, peroxidases (mainly horseradish peroxidase) have been shown to catalyse the coupling of phenolic, substituted phenolic, and aromatic amine compounds [11,12].

A relatively new class of peroxidases, the dye decolourising or DyP-type (EC 1.11.1.19), is a promising group of peroxidases, that have the ability to not only decolourise anthraquinone derived dyes, but to oxidise a wide range of substrates, including veratryl alcohol, β-carotene, lignin and Mn^{2+} [13]. Previously, DyP-type peroxidases were classified into four phylogenetically distinct subfamilies, A-D. A new classification has since been proposed by Yoshida and Sugano [14]: I, P, and V. Group I solely consists of bacterial DyP-type peroxidases that contain a twin arginine translocation (TAT) export signal and are typically 395-445 amino acids in length. Group P do not contain any TAT signals and are smaller than members of group I (287-350 amino acids). Group V predominantly consists of fungal DyP-type peroxidases (with the exception of the DyP-type peroxidases of a cyanobacterium and an *Amycolatopsis* sp. 75iv2) that are more catalytically active than the other two groups, and larger in size (469-526 amino acids). This group of microbial peroxidases are of particular interest since they are considered viable alternatives to plant peroxidases (e.g. horseradish peroxidase) for industrial applications [15].

Actinobacterial peroxidases may therefore offer novel catalytic properties that could be exploited in diverse biotechnological applications. In our previous study [16], *Streptomyces* sp. BSII#1 was shown to be a feasible source for extracellular peroxidase production on medium scale (4.76±0.46 U ml^{-1} from 3 L culture volume). The main aim of the current study was to purify and characterise the peroxidase from *Streptomyces* sp. BSII#1 and to investigate its ability to catalyse coupling reactions between phenolic monomer residues. In addition, genome sequence analyses were performed in order to identify the type of peroxidase(s) produced by strain BSII#1.

Methods and Materials

Chemicals and Reagents

All chemicals and reagents used in this study were purchased from Sigma-Aldrich/Merck-Millipore (South Africa), unless otherwise specified.

The Enzyme-producing Strain

The peroxidase-producing strain, *Streptomyces* sp. BSII#1 [16] was maintained on solid media [Yeast extract Malt extract agar (YEME), pH 7.4] [17] and as 20% (v/v) glycerol stocks at -20°C and -80°C.

Crude Enzyme Preparation

Peroxidase production by *Streptomyces* sp. BSII#1 and preparation of the crude enzyme was carried out in bubble reactors as described in Musengi et al. [16]. Centrifugation (10 000 x*g* for 5 minutes at room temperature) was used to remove the cell mass and to harvest the culture medium (crude extract).

Assays and Statistical Analyses

Peroxidase activity was measured using the 2,4-dichlorophenol (2,4-DCP) assay [18] with the exception that 100 mM Tris-HCl buffer (pH 8.0) was used as the buffer. The reaction was initiated by the addition of H_2O_2 and the increase in absorbance (ε_{510} = 21.647 mM^{-1} cm^{-1}) was monitored for 5 min on a SpectraMax PLUS 384 microtiter plate reader (Molecular Devices, San Jose, California). One unit (U) of peroxidase activity was defined as the amount of enzyme required for the oxidation of 1 µmol of substrate (2,4-DCP) in 1 min. Protein concentration assays were performed in microtitre format according to the manufacturer's instructions for the Bradford's assay reagent (Sigma). All assay readings were performed in triplicate, using two biological repeats. Univariate analysis of variance (Univariate ANOVA) followed by Bonferroni post hoc tests were used to compare results and test for significance (IBM® SPSS® Statistics, Version 21). Only p-values ≤ 0.05 were considered significant.

Purification of Peroxidase

Unless stated otherwise all enzyme purification steps were carried out at 4°C. The pH of the crude extract was adjusted from an initial value of pH 6.8 to pH 2.3 by addition of concentrated HCl. The acidified crude extract was incubated at ambient temperature (25±2°C) for 15 min before centrifugation at 10 000 *g* for 10 min. The pellet was resuspended in 5 ml 100 mM Tris-HCl buffer (pH 8.0) for complete dissolution of the pellet ('acid fraction'). Ten volumes of ice-cold acetone were added to the acid fraction and the mixture was incubated at -20°C for at least 12 h before centrifugation at 10 000 *g* for 10 min. The resultant supernatant was discarded, and the pellet was resuspended in 5 ml 100 mM Tris-HCl buffer (pH 8.0) to enable complete dissolution ('acetone fraction'). The acetone fraction was filtered through Amicon® Ultracel®-30K centrifugal filters (30 000 MWCO; 7 500 *g* for 30 min). The resultant filtrate was designated the 'ultrafiltrate fraction'.

SDS-PAGE analysis

Peroxidase samples (20 µl) were mixed with 4 µl 6x sample loading buffer [375 mM Tris-HCl pH 6.8, 6% (w/v) SDS, 48% (v/v) glycerol, 9% (v/v) 2-mercaptoethanol, and 0.03% (w/v) bromophenol blue]. The samples were boiled for 15 min and allowed to cool. Gels and running buffers were prepared as per the manufacturer instructions for the Mini-PROTEAN® Tetra Cell Gel System (Biorad). Samples (and PageRuler prestained protein ladder [ThermoScientific]) were loaded in lanes on a 12% resolving gel and run at 180 V until the dye front had reached the bottom of the gel. The gel was stained with PageBlue™ Coomassie stain (Fermentas). Staining was allowed to proceed on a rocking shaker overnight and excess stain was removed by washing the gel with distilled water for at least 10 min.

Characterisation of Purified Peroxidases

All characterisation studies were conducted using the ultrafiltration fraction obtained from the acid/acetone purification approach.

Optimum pH, Substrate Range and Optimum Temperature

The substrate range of the purified peroxidase was determined (at 25±2°C) using the following substrates, each at a final concentration of 1 mM and at pH 3, 5, 7 and 9: 2,2'-azino-bis(3-ethylbenzothiazoline-6-sulphonic acid) (ABTS), 2,4-DCP, 2,6-dimethoxyphenol (2,6-DMP), 3-hydroxyanthranilic acid (3-HAA), 4-methylcatechol, 4-*tert*-butylcatechol (4-TBC), caffeic acid, catechol, guaiacol, L-3,4-dihydroxyphenylalanine (L-DOPA), L-tyrosine, *o*-aminophenol, *p*-cresol, phenol, pyrogallol, resorcinol and syringaldazine. In addition, the optimum pH for the oxidation of 2,4-DCP was determined from pH 3 to 9, in increments of 0.5 pH units (sodium acetate buffer pH 3.0 – 5.5; potassium phosphate buffer pH 6.0 – 7.5 and Tris-HCl buffer pH 8.0 – 9.0). The oxidation of 2,4-DCP by the partially purified peroxidase at different temperatures (ranging from 5°C to 80°C at 5°C intervals) was monitored at 510 nm using a UV/VIS Lambda 25 spectrophotometer with a PTP-6+6 Peltier system for temperature control (PerkinElmer, South Africa). The peroxidase was suspended in 100 mM Tris-HCl buffer (pH 8.0) and the optimum temperature for peroxidase activity was determined using the 2,4-DCP assay at pH 8.0.

Thermostability

The partially purified enzyme was incubated in a Corning LSE^{TM} digital dry bath at temperatures ranging from 30 to 80°C (10°C increments) for 10, 20, 30 and 60 min, and immediately cooled on ice. The control sample was incubated on ice throughout the duration of the experiments and had no further treatments applied. The temperature stability of the peroxidase in 100 mM Tris-HCl buffer (pH 8.0) and in 100 mM potassium phosphate buffer (pH 8.0) was determined. Once cool, residual peroxidase activity was measured at ambient temperature (25±2°C) using the 2,4-DCP assay.

pH Stability

Sodium acetate buffer (pH 3.0 – 5.5), potassium phosphate buffer (pH 6.0 – 7.5) and Tris-HCl buffer (pH 8.0 – 9.0) were used at 0.5 pH unit increments in the specified pH range. The purified peroxidase was mixed with equal amounts of each buffer (100 mM concentration) and incubated at 4°C for 24 h and the residual peroxidase activity measured using the 2,4-DCP assay at 25±2°C.

Effects of Inhibitors, Reducing Agents, Metal Ions and Organic Solvents

The ability of the peroxidase to oxidise 2,4-DCP in the presence of 0 to 50 mM of the following compounds was assessed: ethylenediaminetetraacetic acid (EDTA), H_2O_2, L-cysteine, NaCl, *p*-arbutin, sodium ascorbate, sodium azide, sodium dodecylsulphate (SDS) and sodium metabisulphite. The effect of metal ions (Ca^{2+}, Co^{2+}, Cu^{2+}, Fe^{2+}, Mg^{2+}, Mn^{2+} and Zn^{2+}; each at 0.1, 0.5, 1, 2, and 5 mM concentrations) was also determined. The enzyme sample was incubated in the presence of the compound or metal ion for 1 h before assaying for peroxidase activity at 25±2°C and pH 8.0. Results were compared to the control enzyme activity where no inhibitor or metal ions were added. The effect of organic solvents [ethanol, methanol, acetone, acetonitrile, dimethylsulfoxide (DMSO) and 2-propanol] on the ability of the peroxidase to oxidise 2,4-DCP was assessed. The organic solvent was

added to the 2,4-DCP assay mix at 10, 20, 30 and 40% v/v concentration prior to performing the assay at 25±2°C and pH 8.0. The reference control did not contain an organic solvent.

Enzyme Kinetics

The kinetic parameters V_{max} and K_m were determined for the oxidation of 2,4-DCP using non-linear regression analysis (Michaelis-Menton). Data was analysed using Prism 8 for macOS (version 8.4.3). The enzyme concentration was kept constant at 0.1 U ml^{-1} and the concentration of 2,4-DCP was varied (0-10 mM). Assays were performed at ambient temperature (25±2°C) and pH 8.0.

Spectral Characteristics

A complete wavelength scan (200 nm to 700 nm) of the peroxidase from *Streptomyces* sp. BSII#1 (ultrafiltrate fraction) was performed using a Lambda 25™ UV/VIS spectrophotometer (PerkinElmer, South Africa).

Dye Decolourisation Assays

To determine the ability of the peroxidase to decolourise dyes, 100, 75, 50, 25, 10, and 1 μM solutions of each dye were prepared in 50 mM citrate buffer (pH 3.0), 50 mM sodium acetate buffer (pH 5.0), 50 mM potassium phosphate buffer (pH 8.0) and 50 mM Tris-HCl buffer (pH 9.0). Two hundred microliters of dye solution and 50 μl 50 mM H_2O_2 (prepared in the respective buffers) were dispensed into a 96 well microtitre plate in triplicate and 50 μl of a 1 U ml^{-1} enzyme solution was added to each well. The decrease in absorbance was monitored over a period of 90min, as well as 24 h at ambient temperature (25±2°C). Oxidation of Reactive Blue 4 (anthraquinone dye) was monitored at 597 nm (ε = 4 200 M^{-1} cm^{-1}), Reactive Black 5 (azo dye) at 598 nm (ε = 37 200 M^{-1} cm^{-1}), and Azure B (thiazine dye) at 605 nm (ε = 8 700 M^{-1} cm^{-1}).

Liquid Chromatography-Mass Spectrometry (LC-MS) analysis of purified enzyme fraction

LC-MS analysis was performed on a Dionex HPLC system (Dionex Softron, Germering, Germany) equipped with a binary solvent manager and auto-sampler, coupled to a Bruker ESI Q-TOF mass spectrometer (Bruker Daltonik GmbH, Germany). The enzyme fraction was separated by reversed phase chromatography on a Sunfire C18 column 5 μm; 4.6 × 150 mm (Waters, Dublin, Ireland), using gradient elution at a flow rate of 0.5 ml min^{-1}, an injection volume of 10 μl and an oven temperature of 40°C. The gradient was set up as follow: 98 % A to 40 % A (60 min); 40 % A to 98 % A (60 - 60.1 min); 98 % A (60.1 - 80 min), where solvent A refers to 0.1 % formic acid and solvent B refers to acetonitrile. MS spectra were acquired in positive mode using the full scan mode with dual spray for reference mass solution. Electrospray voltage was set to -3500 V. The dry gas flow was set to 8 l min^{-1} with a temperature of 200°C and the nebulizer gas pressure was set to 17.5 psi.

Genomic DNA isolation, genome sequencing and sequence analyses

Streptomyces albidoflavus BSII#1 was cultivated in YEME liquid media (10 d at 30°C, 160 rpm) [13]. Genomic DNA was isolated using the method described by Mandel and Marmur [19]. An Illumina MiSeq sequencer was used to sequence the genome (NGS Facility, University of the Western Cape). The genome was assembled using the A5-miseq pipeline [20] and annotated using the online server, Rapid Annotations using Subsystems Technology (RAST) [21]. This Whole Genome Shotgun project

has been deposited at DDBJ/ENA/GenBank under the accession SCDQ00000000. The version described in this paper is version SCDQ01000000. To confirm the assignment of strain BSII#1 as a *S. albidoflavus* strain, all *S. albidoflavus* genome sequences were downloaded from EzBiocloud [22] and analysed using the average nucleotide identity (ANI), average amino acid identity (AAI) (http://enve-omics.ce.gatech.edu/) [23] and digital DNA-DNA hybridisation online tools (http://ggdc.dsmz.de/) [24].

Peroxidase sequence analyses

The annotated genome was analysed for the presence of genes encoding for peroxidases. The gene sequences were submitted to BLAST to confirm their identity and evaluated for signal peptides that allow for secretion (PSORTb 3.0 analysis; www.psort.org/psortb/; SignalP 4.0; http://www.cbs.dtu.dk/services/SignalP/) [25,26]. SnapGene® Viewer 5.1.5 was used to determine the amino acid content, MW and pI of the secreted dye decolourising peroxidase (DyP). The sequence was also analysed by protein BLASTp [27] to identify related peroxidase sequences. The protein sequences of known DyP-type peroxidases were downloaded from NCBI for phylogenetic analysis: sequences representing the different DyP-type classes were aligned using the alignment function of MEGA 7 [28] and used to generate a Neighbor-Joining tree [29]. In addition, an amino acid sequence alignment of representative DyP-type peroxidases (class I only) was performed using T-Coffee [30,31] and was visualised using SnapGene® Viewer 5.1.5 .

Coupling Reactions and LC-MS Analysis of Coupling Products

The potential of the partially purified peroxidase to catalyse the oxidative coupling of phenolic monomers was evaluated. Reactions consisted of the enzyme (final concentration of 1 U ml^{-1}), two phenolic monomer substrates (final concentration 2 mM each and dissolved in ethanol), H_2O_2 (final concentration 0.37 mM) and 100 mM ammonium bicarbonate buffer (pH 8.0) in a total reaction volume of 650 µl. The substrates tested consisted of combinations of catechin, catechol or guaiacol with trans-cinnamic acid, chlorogenic acid, *p*-coumaric acid, ferulic acid, cinnamyl alcohol, syringaldazine or with each other. The reactions were initiated upon addition of H_2O_2 and were incubated at 30°C for 10 min. The reactions were terminated by the addition of 650 µl ice-cold methanol (99.8%) and placed on ice for 30 min before centrifugation at 4°C, 9 500 *g* for 10 min. The supernatant was collected from each reaction tube and stored at 4°C in HPLC glass vials prior to analysis by LC-MS.

LC-MS analysis of the coupling products was performed using the gradient system: 98% A to 0% A (20 min); 0% A to 98% A (20 - 21 min); 98% A (21 - 25 min); where solvent A was 0.1% formic acid and solvent B was acetonitrile. The injection volume was 10 µl, the flow rate was set at 0.8 ml min^{-1} and the column oven temperature was set at 30°C. The products were separated by reversed phase chromatography on a C18 column 5 µm; 4.6 × 150 mm (Thermo Fischer Scientific, Bellefonte, USA). MS spectra were acquired in negative mode using the full scan mode with dual spray for reference mass solution. Electrospray voltage was set to +3500 V, and the dry gas flow was set to 9 l min^{-1} with a temperature of 300 °C; nebulizer gas pressure was set to 35 psi.

Results

Partial Purification of the Peroxidase

The crude extracellular enzyme extract was yellow/yellow-brown in colour. After acidification and the removal of precipitates, the acid fraction appeared to be red to red-brown, and the final ultrafiltrate fraction was reddish-pink. Acidification resulted in doubling of the purification factor with only a 10% drop in the yield, while ultrafiltration improved the purity of the acetone fraction almost 20 times (Table 1). Even though these purification steps resulted in a great loss of protein, the purity was greatly increased allowing for subsequent characterisation and application of the enzyme. SDS-PAGE analysis (Figure S1) indicated that purification to at least near homogeneity was accomplished and that the enzyme is a dimeric protein with an approximate molecular mass of 50.5 kDa.

Optimum pH, Substrate Range and Optimum Temperature

The oxidation of 2,4-DCP by the partially purified peroxidase was tested over the range from pH 3.0 to 8.5. The apparent maximum 2,4-DCP oxidation occurred at pH 8.0 (Figure 1a). However, there was no significant difference in the oxidation rate from pH 5.0 to pH 8.5 ($p>0.05$), with the exception of the anomalous reaction rate at pH 6.0. Apart from 2,4-DCP, the peroxidase was also able to oxidise a wide range of substrates (Table 2), with highest activity detected for 4-TBC, followed by *o*-aminophenol and catechol. The optimum temperature for maximum oxidation of 2,4-DCP by the peroxidase was tested from 5 to 80°C. There was a large variation in activity between replicates at higher temperatures, particularly between 40 and 60°C (Figure 1b), probably due to substrate instability. The apparent optimum temperature for the peroxidase appeared to be 60°C but it was not possible to statistically determine an accurate optimal temperature for activity. However, it was evident that the enzyme was active over a wide temperature range (from 5°C to 80°C).

Thermostability

The peroxidase was suspended in two buffering systems for the thermostability test: 100 mM Tris-HCl buffer (pH 8.0) (Figure 2a) and 100 mM potassium phosphate buffer (pH 8.0) (Figure 2b). ANOVA and post-hoc Bonferroni analysis of the results presented in Figure 2a indicated that while there was a similar significant decrease in activity (20-30%) of the enzyme suspended in Tris-HCl buffer (pH 8.0) after 10 min incubation at all temperatures tested ($p<0.05$), there was no further loss of activity with up to 60 min incubation at temperatures from 30 to 80°C ($p>0.05$). In contrast, the enzyme suspended in potassium phosphate buffer (pH 8.0) (Figure 2b) showed no significant change in activity after incubation at temperatures from 30 to 50°C for up to 60 min. However, there were significant differences between activity in the control and activity after incubation at 60, 70 and 80°C for even the shortest incubation period tested (10min).

pH Stability

The residual activity of the enzyme was determined after a 24 h incubation period in buffers with varying pH (pH 3.0 to pH 9.0). Peroxidase activity appeared to be most stable from pH 5.0 to 9.0 with maximum residual activity observed when the enzyme was incubated at pH 9.0, where 81% activity was retained after 24 h (Figure 3). There was total loss of activity after the peroxidase was incubated at pH 3.0, 3.5 and 4.0, and >90% loss of activity at pH 4.5.

Effects of Inhibitors, Reducing Agents, Metal Ions and Organic Solvents

The partially purified peroxidase was incubated in the presence of various inhibitors, reducing agents and metal ions for 60 min, after which the residual activity was measured. The peroxidase was most sensitive to its co-factor, H_2O_2, where complete inhibition was observed at 0.05 mM and significant inhibition (42%) was also noted at the lowest concentration tested (0.01 mM) (Table 3). Sodium metabisulphite, L-cysteine, sodium ascorbate and *p*-arbutin were expected to react with groups within the protein structure, resulting in either activation or inhibition of peroxidase activity. All four compounds resulted in inhibition of peroxidase activity, with complete inhibition occurring after 60 min of incubation with 0.1 mM L-cysteine (Table 3). However, the peroxidase showed considerable resistance to inhibition by sodium azide (Table 3), with no significant loss of activity in the presence of up to 2 mM sodium azide and retaining 32% activity after incubation with 50 mM sodium azide for 60 min. Most of the metal ions tested showed either no effect or an inhibitory action on the activity of the peroxidase (Figure 4), except for copper, which enhanced activity. Zinc, calcium and magnesium ions had no significant effect on activity of the peroxidase, while cobalt, iron and manganese ions had the greatest inhibitory effect. There was a significant decrease in activity relative to the control at all concentrations of each solvent tested, even at the lowest solvent concentrations used (10% v/v) (Figure 5). The simple alcohols showed the least inhibitory effect at low concentrations, while the presence of acetonitrile resulted in the greatest inhibition at all the concentrations tested (Figure 5).

Enzyme Kinetics

The peroxidase from *S. albidoflavus* BSII#1 was shown to follow Michaelis-Menten kinetics, with respect to 2,4-DCP oxidation (data not shown). Analysis of derivative plots of the substrate concentration versus velocity curve indicated K_m and V_{max} values of 0.95 mM and 0.12 mmol min^{-1}, respectively (Table S1).

Spectral Characteristics

The complete wavelength scan of the partially purified peroxidase (Figure S2) indicated an absorption peak at 400 nm, corresponding to the Soret band, which is characteristic of haem peroxidases. The purified protein was analysed by LC-MS to determine the size. The chromatogram showed a single large peak (at 48 min) with only two minor peaks (32 min and 65 min) suggesting that the enzyme was almost completely purified (Figure S3a). The 48 min peak (presumed to be the peroxidase of interest) was analysed by mass spectrometry (Figure S3b) which showed that the size of the protein was 46 kDa as interpreted according to Mann et al. [32].

Dye Decolourisation

Dye decolourisation was observed for all three dyes tested, with optimal decolourisation taking place at pH8. After 24 h of incubation, the peroxidase most effectively decolourised reactive blue 4 (RB4), followed by reactive black 5 (RB5) and Azure B (Figure 6).

Genome Sequence Analysis, Peroxidase Sequence Analysis, and Functional Expression

Streptomyces albidoflavus BSII#1 has a genome size of 7019108 bp (1057 contigs; N50: 11575) and a G+C content of 73.01%. Even though the digital DNA-DNA hybridisation tool predicted that strain

BSII#1 could represent a novel species (66.5% vs *S. albidoflavus* NRRL B-1271^T), the ANI and AAI analysis of the BSII#1 genome sequence and the type strain *S. albidoflavus* NRRL B-1271^T, confirmed the assignment of strain BSII#1 as a *S. albidoflavus* strain (Figure S4; ANI: 96.5%; AAI: 97.41%) [23].

Six peroxidase sequences were identified in the genome of *S. albidoflavus* BSII#1. SignalP 4.1 analysis showed that only the DyP-type peroxidase contains a signal peptide sequence indicating secretion. BLASTp analysis also predicted the presence of a TAT sequence, while PSORTb analysis indicated that there is a 97.3% chance that this protein is an extracellular protein. The predicted DyP-type peroxidase is 414 aa in length, with a predicted MW of 45.39 kDa (which corresponds with the size determined by LC-MS) and pI of 6.69. Phylogenetic analysis of known DyP-type peroxidases and the BSII#1 DyP-type peroxidase showed that this peroxidase belongs to class I (formerly class A; Figure S5). BLASTp analysis showed 100% sequence similarity (and coverage) to other *Streptomyces* DyP-type peroxidases (WP_023418253.1) [14]. Amino acid sequence alignment (Figure S6) confirmed the presence of highly conserved amino acid residues involved in haem co-ordination and the formation of the hydrogen peroxide binding pocket. In addition, the conserved GXXDG motif is also present [14]. To confirm functional expression of this peroxidase under the experimental conditions described in this study (see Supplementary Material), total RNA was isolated from the peroxidase-producing strain, converted to cDNA and used as a template in PCR using DyP-type peroxidase-specific primers. A 352bp amplicon was obtained and confirmed to be the predicted DyP-type peroxidase present in the genome of strain BSII#1. The amino acid and nucleotide sequences for the BSII#1 DyP-type peroxidase are provided in the supplementary information.

Coupling Reactions

The ability of the partially purified peroxidase from *S. albidoflavus* BSII#1 to catalyse the coupling of phenolic monomers was assessed under non-optimised conditions. LC-MS results indicated that the peroxidase was able to catalyse coupling of a number of different phenolic monomer pairs (Table S2). HPLC results indicated that significant coupling occurred between catechin and guaiacol, and between catechin and catechol (based on peak areas, data not shown). Based on similar work on flavolignans [33-35], the structures of the coupling products between catechin and guaiacol or catechol were proposed (Figure 7). However, the work by Gažák et al. [33] also showed that the major products were likely C-C dimers due to the stability of C–C bonds [36] and their lower heat of formation [37].

Discussion

Peroxidases are versatile enzymes with numerous uses. Most peroxidase studies have focussed on fungal and plant (notably horseradish) peroxidases. However, actinobacteria could be an alternative and viable source of industrially useful peroxidases with novel properties [16,38]. While bacterial peroxidase production is often lower than fungi, these peroxidases could offer other useful characteristics, for example their substrate specificity or different optimal parameters for use. This study therefore focused on the production, characterisation, and application of a DyP-type peroxidase produced by a *S. albidoflavus* strain.

Common protein purification methods tested (such as salting out) resulted in very low peroxidase recovery yields (data not shown). Although acidification has not previously been used to precipitate actinobacterial peroxidases, this study showed that it was an effective initial step in purification. The ultrafiltration step also proved effective in improving the purity of the enzyme. While the purification resulted in a drastic decrease in protein concentration/loss of protein, there was a 20-fold increase in purity – which was important for this study in order to show it was the actions of this enzyme that catalysed the coupling reactions. The red colour in the ultrafiltrate fraction could be indicative of the association of the enzyme with a chromogenic cofactor [39,40]. The characteristic peak (Soret band) at approximately 400 nm is attributed to the presence of a haem moiety within the enzyme structure. The peroxidase from *S. albidoflavus* BSII#1 is therefore suggested to be a haem peroxidase.

Actinobacterial peroxidases typically exhibit pH optima in the alkaline region and, while the peroxidase from *S. albidoflavus* BSII#1 shows an apparent optimal activity at pH 8.0, it also showed similar activity in the pH range 5.0 to 8.5 (i.e. in the acidic, neutral and alkaline range). Typical peroxidase substrates such as ABTS, phenol and pyrogallol were oxidised and the enzyme showed a wide substrate range. The ability of actinobacterial peroxidases to oxidise a wide range of substrates has previously been reported, for example, the peroxidase from *Streptomyces albus* ATCC 3005, showed activity with L-DOPA, 2,4-DCP and several other chlorophenols [18]. The peroxidase was most stable after incubation at alkaline pH, which agrees with the general finding that actinobacterial peroxidases tend to be more stable under alkaline pH conditions [41].

Contrary to statements made in the majority of publications on DyP-type peroxidases, dye decolourisation is not limited to anthraquinone dyes (e.g. RB4 decolourisation by the DyP-type peroxidase produced by *Rhodococcus jostii* RHA1) [42]. Two bacterial DyP-type peroxidases have shown the ability to decolourise the azo dye, Mordant black 9 (BsDyP – *Bacillus subtilis* and PpDyP – *Pseudomonas putida* MET94), while two fungal DyP-type peroxidases (*Auricularia auricula-judae* and *Irpex lacteus*) and one bacterial (*Escherichia coli*) DyP-type peroxidase have been reported to decolourise the azo dye, RB5 [42]. In the present study, the *S. albidoflavus* BSII#1 peroxidase showed the ability to decolourise RB4, RB5 and Azure B to various degrees.

The concept of 'optimum temperature of enzymes' has been challenged as one of dubious validity and limited value because the apparent optimum temperature arises from an unknown mix of thermal stability and temperature coefficient and is dependent upon assay duration [43]. The optimum temperature of an enzyme has been described as a non-intrinsic parameter whose dependence on a variety of other factors may not make it a very useful point of reference. In this study, the enzyme was relatively stable, retaining >60% activity after incubation at high temperatures (up to 80°C for up to 60 min) in Tris-HCl buffer (pH 8.0); however, the activity at temperatures >40°C was highly variable. The variance may be attributed to instability of the enzyme or other reaction components. Since the peroxidase appeared to be stable at temperatures below 40°C (Figure 1b), the variability was most probably due to non-specific reactions between assay components at the elevated temperatures. The instability of the assay mix at elevated temperatures in the present study illustrated the point of the limited value of the concept of an optimal

temperature. It is more useful to determine the optimal temperature for the specific reaction tested. Furthermore, the analyses indicate that while the enzyme is fairly stable at high temperatures, the suspension buffer plays a role in the thermostability. The inference is that for higher temperature applications (greater than 50°C), using Tris–HCl buffer (pH 8.0) may be preferable over potassium phosphate buffer (pH 8.0) as this enhanced the thermostability of the peroxidase. According to Reineke et al. [44], the pH of certain buffers is affected with an increase in temperature. While phosphate buffer systems seem to be able to maintain their pH with change in temperature, the pH of Tris-HCl buffers decreases with increasing temperature, with a pH of approximately 6.8 at 80°C [44]. This combination of increasing temperature and decreasing pH therefore seemed to result in enhancing the thermostability of the enzyme.

Although H_2O_2 is a cofactor for peroxidases, it inhibited the peroxidase from *S. albidoflavus* BSII#1 after incubation with even low (0.01-0.05 mM) H_2O_2 concentrations (suicide inactivation phenomenon) [45]. The duration of the exposure of the enzyme to H_2O_2 was the most likely reason for significant inhibition even at very low concentrations. Evidence for this is that the activity of the enzyme was routinely assayed at final H_2O_2 concentrations of 10 mM ($1x10^3$ times the minimum inhibitory concentration) without inhibitory effects being observed. EDTA, SDS and NaCl did not have any significant effect(s) on peroxidase activity at all concentrations tested (0.01 mM to 50 mM) under conditions of the experiment. The other inhibitory compounds tested showed lower levels of inhibition compared to L-cysteine, which could be due to the strong reduction potential of L-cysteine. Inhibition studies using these compounds with actinomycete-derived peroxidases have not been reported and therefore direct comparisons for validation could not be made. Most haem peroxidases are readily inactivated by sodium azide [40,46-50]. For example, in a similar experiment performed under similar conditions, the peroxidase from *Streptomyces* sp. strain AH4 retained 40% of its activity after incubation with 5 mM sodium azide for 60 min [40]. Furthermore, the peroxidase from *Streptomyces* sp. AD001 exhibited 90% inhibition after 30 min exposure to 1 mM sodium azide at 4°C [47]. In this study, the peroxidase from *S. albidoflavus* BSII#1 showed considerable resistance to inhibition by sodium azide (no inhibition after 60 min incubation with 2 mM sodium azide), further indicating the atypical properties of this enzyme.

Some metal ions have been shown to pose similar effects on the peroxidases from different actinomycetes. The peroxidases from *Streptomyces* sp. AM2, *Streptomyces* sp. AH4, and *S. albidoflavus* TN644 were reportedly inhibited to different extents by the presence of 5 mM zinc ions but were induced in the presence of 5 mM calcium, manganese or copper ions [40,50,51]. Induction of activity by copper ions was reported for the peroxidase from *S. albidoflavus* TN644 and *Streptomyces* sp. strain AH4, where a residual activity of 108% and 111%, respectively, after 60 min incubation in the presence of 5 mM $CuCl_2$, was reported [40,51]. Copper ions also induced the activity of the peroxidase from *S. albidoflavus* BSII#1. In contrast to the peroxidase from *Streptomyces* sp. AH4 [40], zinc, calcium and magnesium ions had no significant effect on the activity of the peroxidase from *S. albidoflavus* BSII#1. The effect of a single type of metal ion on peroxidase activity does not appear to be typical for all actinomycete-derived peroxidases and could be dependent on the source organism. Alternatively, the atypical characteristics of the peroxidase of interest could extend to the effect of metal ions. The ability of a peroxidase to exhibit high activity in

the presence of metal ions is considered a useful attribute when considering its potential for industrial application [50]. The potential of the peroxidase from *S. albidoflavus* BSII#1 for use in applications that require metal ion tolerance (e.g. dye decolourisation) is therefore dependent on the identity and concentration of the particular metal ion.

Organic solvents are often used to solubilise starting reagents for catalysis and the efficacy of biocatalytic reactions will depend on the robustness of an enzyme in the presence of organic solvents [52]. Optimisation of enzyme stability in organic solvents generally improves catalytic performance. The majority of natural enzymes are readily denatured and inactivated in the presence of organic solvents [53]. In this regard, the peroxidase under investigation was quite typical.

Comparison of the kinetic properties of the *S. albidoflavus* BSII#1 peroxidase with that of other reported actinobacterial peroxidases, horseradish peroxidase (HRP) and *P. chrysosporium* peroxidase (Table S1) showed that it shares a similar affinity for 2,4-DCP as HRP, which is higher than that of peroxidases from other *Streptomyces* species reported (with the exception of ALiP-P3 and the *S. albidoflavus* TN644 peroxidase; Table S1). The low K_m (high affinity) and high V_{max} values with the substituted phenol substrate are comparable to that of fungal peroxidases and the commercially available peroxidase, HRP, which indicate the potential of this enzyme for industrial application.

Several factors affect the successful coupling of phenolic monomers by an enzyme, including steric hindrance [54]. Catechol and guaiacol are small molecules with a small number of substituents (two). This reduces steric hindrance and increases the chances of coupling. Table S2 shows that the majority of coupling reactions took place between catechin and a second substrate. This could be due to the fact that upon oxidation, catechin does not readily polymerise, which increases the chances of catechin radicals coupling with other molecules. The coupling reactions were performed in an ammonium bicarbonate buffer solution and the enzyme was freely suspended in solution. Since environmental factors within the system (including temperature, pH, medium components, enzyme inhibitors and cofactors) may also influence coupling reactions, optimisation of these factors may significantly increase the yield of the coupling products.

With the ever-decreasing costs of genome sequencing, more sequence information is becoming available, allowing researchers to gain more insight into the distribution of genetic information. In this study, the genome sequencing of strain BSII#1, not only allowed for the identification of the strain to species level (*S. albidoflavus*), but also allowed access to the gene encoding for the peroxidase of interest (DyP-type peroxidase – as confirmed by functional expression). Multiple sequence alignment of the DyP-type peroxidases found in the *S. albidoflavus* genomes showed slight variations in the amino acid sequences (results not shown). The *S. albidoflavus* BSII#1 DyP-type peroxidase exhibited the same amino acid variations as *S. albidoflavus* PVA 94-07, a strain isolated from the marine sponge *Phakellia ventilabrum*, Trondheimfjord, Norway [55]. Without more information on the physicochemical properties of the two environments the isolates were obtained from, it is difficult to explain why these two strains would harbour the same DyP-type peroxidase genes. There is still a great lack of understanding about the biochemical characteristics of DyP-type peroxidases in general. This is further complicated by the fact that there is no standard set of

biochemical analyses recommended for this group of unique peroxidases, making it difficult to assess the potential biological roles of this interesting group of peroxidases.

Conclusions

In this study, a protocol for the purification of the DyP-type peroxidase from *S. albidoflavus* BSII#1 involving acidification, acetone fractionation and ultrafiltration steps, was successfully developed. While acidification has not previously been used in actinobacterial peroxidase purification, it proved to be effective in the purification protocol developed. The purified peroxidase was found to have an approximate molecular mass of 46 kDa (LC-MS analysis; 50.5 kDa by SDS-PAGE), which is within the size range of the predicted DyP-type peroxidase (45.39 kDa) discovered through genome mining. As with other DyP-type peroxidases, it was confirmed that the enzyme is a haem peroxidase, it displays characteristics typical of those described for other actinobacterial peroxidases, was found to be capable of catalysing coupling reactions between several phenolic monomer pairs, and hence has potential for application in organic synthesis. The peroxidase from *S. albidoflavus* BSII#1 showed activity over a wide range of pH and temperature conditions and high tolerance to some typical peroxidase inhibitors (e.g. sodium azide), which are useful characteristics in the search for novel biocatalysts. Future studies will explore the recombinant expression of this enzyme with the aim of exploring application in other fields of organic synthesis and degradation.

Acknowledgements

The authors thank Dr Corrie Uys for her assistance with the statistical analyses and Prof. Don Cowan for his generous donation of soil samples from which *S. albidoflavus* BSII#1 was isolated.

Funding: The authors also acknowledge the National Research Foundation (NRF) of South Africa for funding the project (grant number: UID 105873) and the Water Research Commission (WRC) for the student bursary. Any opinions, findings and conclusions or recommendations expressed in this material are those of the authors and therefore the NRF and WRC do not accept any liability in regard thereto.

Conflict of Interest

The authors declare that they have no conflict of interest.

Additional information can be found in the Supplementary material document.

References

1. A. Hatakka, Lignin-modifying enzymes from selected white-rot fungi- production and role in lignin degradation, FEMS Microbiol. Rev. 13 (1994) 125-135. https://doi.org/10.1111/j.1574-6976.1994.tb00039.x.

2. A. Bhunia, S. Durani, P.P. Wangikar, Horseradish peroxidase catalysed degradation of industrially important dyes, Biotechnol. Bioeng. 72 (2001) 562-567. https://doi.org/10.1002/1097-0290(20010305)72:5<562::AID-BIT1020>3.0.CO;2-S.

3. A.M. Klibanov, Peroxidase-catalyzed removal of phenols from coal conversion waste waters, Science 221 (1983) 259–261. https://doi.org/10.1126/science.221.4607.259-a.

4. J.A. Nicell, K.W. Saadi, I.D. Buchanan, Phenol polymerization and precipitation by horseradish peroxidase enzyme and an additive, Bioresour. Technol. 54 (1995) 5-16. https://doi.org/10.1016/0960-8524(95)00104-2.

5. A. Conesa, P.J. Punt, C.A.M.J.J. van den Hondel, Fungal peroxidases: molecular aspects and applications, J. Biotechnol. 93 (2002) 143-158. https://doi.org/10.1016/S0168-1656(01)00394-7.

6. T. Kudanga, S. Burton, G.S. Nyanhongo, G.M. Guebitz, Versatility of oxidoreductases in the remediation of environmental pollutants, Front. Biosci. (Elite Ed) 4 (2012) 1127-1149. https://doi.org/10.2741/446.

7. J.J. Roberts, P. Naudiyal, K.S. Lim, L.A. Poole-Warren, P.J. Martens, A comparative study of enzyme initiators for crosslinking phenol-functionalized hydrogels for cell encapsulation, Biomater. Res. 20 (2016) 30. https://doi.org/10.1186/s40824-016-0077-z.

8. M. Khanmohammadi, M.B. Dastjerdi, A. Ai, A. Ahmadi, A. Godarzi, A. Rahimi, J. Ai, Horseradish peroxidase-catalyzed hydrogelation for biomedical applications, Biomater. Sci. 6 (2018) 1286-1298. https://doi.org/10.1039/C8BM00056E.

9. M. Nakahata, E. Gantumur, K. Furuno, S. Sakai, M. Taya, Versatility of hydrogelation by dual-enzymatic reactions with oxidases and peroxidase, Biochem. Eng. J. 131 (2018) 1-8. https://doi.org/10.1016/j.bej.2017.12.003.

10. R. Vanella, A. Bazin, D.T. Ta, M.A. Nash, Genetically encoded stimuli-responsive cytoprotective hydrogel capsules for single cells provide novel genotype-phenotype linkage, Chem. Mater. 31 (2019) 1899−1907. https://doi.org/10.1021/acs.chemmater.8b04348.

11. J.A. Akkara, K.J. Senecal, D.L. Kaplan, Synthesis and characterization of polymers produced by horseradish peroxidase in dioxane, J. Polym. Sci. Pol. Chem. 29 (1991) 1561-1574. https://doi.org/10.1002/pola.1991.080291105.

12. A. Cozzolino, A. Piccolo, Polymerization of dissolved humic substances catalysed by peroxidase. Effects of pH and humic composition, Org. Geochem. 33 (2002) 281-294. https://doi.org/10.1016/S0146-6380(01)00160-7.

13. R. Singh, L.D. Eltis, The multihued palette of dye-decolorizing peroxidases, Arch. Biochem. Biophys. 574 (2015) 56-65. https://doi.org/10.1016/j.abb.2015.01.014.

14. T. Yoshida, Y. Sugano, A structural and functional perspective of DyP-type peroxidase family, Arch. Biochem. Biophys. 574 (2015) 49-55. https://doi.org/10.1016/j.abb.2015.01.022.

15. N. Lončar, D.I. Colpa, M.W. Fraaije, Exploring the biocatalytic potential of a DyP-type peroxidase by profiling the substrate acceptance of *Thermobifida fusca* DyP peroxidase, Tetrahedron 72 (2016) 7276-7281. https://doi.org/10.1016/j.tet.2015.12.078.

16. A. Musengi, N. Khan, M. Le Roes-Hill, B.I. Pletschke, S.G. Burton, Increasing the scale of peroxidase production by *Streptomyces* sp. strain BSII#1, J. Appl. Microbiol. 116 (2014) 554-562. https://doi.org/10.1111/jam.12380.

17. E.B. Shirling, D. Gottlieb, Methods for characterization of *Streptomyces* species, Int. J. Syst. Bacteriol. 16 (1966) 313-340. https://doi.org/10.1099/00207713-16-3-313.

18. V.T. Antonopoulos, M. Hernandez, M.E. Arias, E. Mavrakos, A.S. Ball, The use of extracellular enzymes from *Streptomyces albus* ATCC 3005 for the bleaching of eucalyptus Kraft pulp, Appl. Microbiol. Biotech. 57 (2001) 92-97. https://doi.org/10.1007/s002530100740.

19. M. Mandel, J. Marmur, Use of ultraviolet absorbance-temperature profile for determining the guanine plus cytosine content of DNA, in: L. Grossman, K. Moldave (Eds.), Methods in Enzymology Vol. 12, Academic Press, New York, 1968, pp. 195 – 206.

20. D. Coil, G. Jospin, A.E. Darling, A5-miseq: an updated pipeline to assemble microbial genomes from Illumina MiSeq data, Bioinformatics 31 (2015) 587-589. https://doi.org/10.1093/bioinformatics/btu661.

21. R.K. Aziz, D. Bartels, A.A. Best, M. DeJongh, T. Disz, R.A. Edwards, K. Formsma, S. Gerdes, E.M. Glass, M. Kubal, F. Meyer, G.J. Olsen, R. Olson, A.L. Osterman, R.A. Overbeek, L.K. McNeil, D. Paarman, T. Paczian, B. Parrello, G.D. Pusch, C. Reich, R. Stevens, O. Vassieva, V. Vonstein, A. Wilke, O. Zagnitko, The RAST server: rapid annotations using subsystems technology, BMC Genomics 9 (2008) 75. https://doi.org/10.1186/1471-2164-9-75.

22. S.H. Yoon, S.M. Ha, S. Kwon, J. Lim, Y. Kim, H. Seo, J. Chun, Introducing EzBioCloud: A taxonomically united database of 16S rRNA and whole genome assemblies, Int. J. Syst. Evol. Microbiol. 67 (2017) 1613-1617. https://doi.org/10.1099/ijsem.0.001755.

23. R.L.M. Rodriguez, K.T. Konstantinidis, The enveomics collection: a toolbox for specialized analyses of microbial genomes and metagenomes, PeerJ Preprints 4 (2016) e1900v1. https://doi.org/10.7287/peerj.preprints.1900v1.

24. J.P. Meier-Kolthoff, A.F. Auch, H.-P. Klenk, M. Göker, Genome sequence-based species delimitation with confidence intervals and improved distance functions, BMC Bioinformatics 14 (2013) 60. https://doi.org/10.1186/1471-2105-14-60.

25. N.Y. Yu, J.R. Wagner, M.R. Laird, G. Melli, S. Rey, R. Lo, P. Dao, S.C. Sahinalp, M. Ester, L.J. Foster, F.S.L. Brinkman, PSORTb 3.0: improved protein subcellular localization prediction with refined localization subcategories and predictive capabilities for all prokaryotes, Bioinformatics 26 (2010) 1608–1615. https://doi.org/10.1093/bioinformatics/btq249.

26. H. Nielsen, Predicting Secretory Proteins with SignalP, in: D. Kihara (Ed.), Protein Function Prediction, Methods in Molecular Biology vol. 1611, Humana Press, New York, 2017, pp. 59-73. https://doi.org/10.1007/978-1-4939-7015-5_6.

27. S.F. Altschul, W. Gish, W. Miller, E.W. Myers, D.J. Lipman, Basic local alignment search tool, J. Mol. Biol. 215 (1990) 403-410.

28. S. Kumar, G. Stecher, K. Tamura, MEGA7: Molecular Evolutionary Genetics Analysis version 7.0 for bigger datasets, Mol. Biol. Evol. 33 (2016) 1870-1874. https://doi.org/10.1093/molbev/msw054.

29. N. Saitou, M. Nei, The neighbor-joining method: a new method for reconstructing phylogenetic trees, Mol. Biol. Evol. 4 (1987) 406-425. https://doi.org/10.1093/oxfordjournals.molbev.a040454.

30. L. Zimmermann, A. Stephens, S.Z. Nam, D. Rau, J. Kübler, M. Lozajic, F. Gabler, J. Söding, A.N. Lupas, V. Alva, A completely reimplemented MPI bioinformatics toolkit with a new HHpred server at its core, J. Mol. Biol. 430 (2018) 2237-2243. https://doi.org/10.1016/j.jmb.2017.12.007

31. C. Notredame, D.G. Higgins, J. Heringa, T-Coffee: A novel method for fast and accurate multiple sequence alignment. J. Mol. Biol. 302 (2000) 205-217. https://doi.org/10.1006/jmbi.2000.4042.

32. M. Mann, C.K. Meng, J.B. Fenn, Interpreting mass spectra of multiply charged ions, Anal. Chem. 61 (1989) 1702-1708. https://doi.org/10.1021/ac00190a023.

33. R. Gažák, P. Sedmera, M. Marzorati, S. Riva, V. Křen, Laccase-mediated dimerization of the flavonolignan silybin, J. Mol. Catal. B: Enzym. 50 (2008) 87-92. https://doi.org/10.1016/j.molcatb.2007.09.005.

34. P. Widsten, C. Heathcote, A. Kandelbauer, G. Guebitz, G.S. Nyanhongo, P.E. Nugroho, T. Kudanga, Enzymatic surface functionalisation of lignocellulosic materials with tannins for enhancing antibacterial properties, Process Biochem. 45 (2010) 1072-1081. https://doi.org/10.1016/j.procbio.2010.03.022.

35. P. Gavezzotti, E. Vavříková, K. Valentová, G. Fronza, T. Kudanga, M. Kuzma, S. Riva, D. Biedermann, V. Křen, Enzymatic oxidative dimerization of silymarin flavonolignans, J. Mol. Catal. B: Enzym. 109 (2014) 24-30. https://doi.org/10.1016/j.molcatb.2014.07.012.

36. J.S. Lupoi, S. Singh, R. Parthasarathi, B.A. Simmons, R.J. Henry, Recent innovations in analytical methods for the qualitative and quantitative assessment of lignin, Renew. Sust. Energ. Rev. 49 (2015) 871-906. https://doi.org/10.1016/j.rser.2015.04.091.

37. P.J.S. Valencia, L.E.B. Marinez, Lignin in the restoration of the cultural heritage, Revista Colombiana de Física 37 (2005) 106-109.

38. M. Le Roes-Hill, N. Khan, S.G. Burton, Actinobacterial peroxidases: and unexplored resource for biocatalysis, Appl. Biochem. Biotechnol. 164 (2011) 681-713. https://doi.org/10.1007/s12010-011-9167-5.

39. E. Van Bloois, D.E.T. Pazmino, R.T. Winter, M.W. Fraaije, A robust and extracellular heme-containing peroxidase from *Thermobifida fusca* as a prototype of a bacterial peroxidase superfamily, Appl. Microbiol. Biotech. 86 (2010) 1419-1430. https://doi.org/10.1007/s00253-009-2369-x.

40. D. Fodil, B. Jaouadi, A. Badis, Z. Jaouadi, N. Fatma, Z. Ferradji, S. Bejar, H. Boutoumi, A thermostable humic acid peroxidase from *Streptomyces* sp. strain AH4: Purification and biochemical characterization, Bioresour. Technol. 111 (2012) 383-390. https://doi.org/10.1016/j.biortech.2012.01.153.

41. M. Tuncer, A. Kuru, N. Sahin, M. Isikli, K. Isik, Production and partial characterisation of extracellular peroxidase produced by *Streptomyces* sp. F6616 isolated in Turkey, Ann. Microbiol. 59 (2009) 323-334. https://doi.org/10.1007/BF03178335.

42. E. Strittmatter, D.A. Plattner, K. Piontek, Dye-decolorizing peroxidase (DyP), in: Encyclopedia of Inorganic and Bioinorganic Chemistry, R.A. Scott (Ed.) 2014. doi: 10.1002/9781119951438.eibc2276.

43. R.M. Daniel, M.J. Danson, R. Eisenthal, The temperature optima of enzymes: a new perspective on an old phenomenon, Trends Biochem. Sci. 26 (2001) 223-225. https://doi.org/10.1016/s0968-0004(01)01803-5.

44. K. Reineke, A. Mathys, D. Knorr, Shift of pH-value during thermal treatments in buffer solutions and selected foods, Int. J. Food. Prop. 14 (2011) 870-881. https://doi.org/10.1080/10942910903456978.

45. B. Valderrama, M. Ayala, R. Vasquez-Duhalt, Suicide inactivation of peroxidases and the challenge of engineering more robust enzymes, Chem. Biol. 9 (2002) 555-565. https://doi.org/10.1016/S1074-5521(02)00149-7.

46. A. Rob, M. Hernandez, A.S. Ball, M. Tuncer, M.E. Arias, M.T. Wilson, Production and partial characterization of extracellular peroxidases produced by *Streptomyces avermitilis* UAH30, Appl. Biochem. Biotech. 62 (1997) 159-174. https://doi.org/10.1007/BF02787992.

47. J. Jeong-Ho, Y.J. Han, T.G. Kang, E.S. Kim, S.K. Hong, B.C. Jeong, Purification and characterisation of 2,4-dichlorophenol oxidising peroxidase from *Streptomyces* sp. AD 001, J. Microbiol. Biotechnol. 12 (2002) 972-978.

48. M. Ramachandra, D.L. Crawford, G. Hertel, Characterisation of an extracellular lignin peroxidase of the lignocellulolytic actinomycete *Streptomyces viridosporus*, Appl. Environ. Microbiol. 54 (1988) 3057–3063. PMCID: PMC204427, PMID: 3223769.

49. A. Mliki, W. Zimmerman, Purification and characterization of an intracellular peroxidase from *Streptomyces cyaneus*, Appl. Environ. Microbiol. 58 (1992) 916-919. PMID: 1315499, PMCID: PMC195355.

50. D. Fodil, A. Badis, B. Jaouadi, N. Zaraî, F.M. Ferradji, H. Boutoumi, Purification and characterization of two extracellular peroxidases from *Streptomyces* sp. strain AM2, a decolorizing actinomycete responsible for the biodegradation of natural humic acids, Int. Biodeterior. Biodegrad. 65 (2011) 470-478. https://doi.org/10.1016/j.ibiod.2011.01.009.

51. B. Jaouadi, H. Rekik, A. Badis, N.Z. Jaouadi, M. Belhoul, M. Hmidi, S. Kourdali, D. Fodil, S. Bejar, Production, purification, and characterisation of a highly thermostable and humic acid biodegrading peroxidase from a decolorizing *Streptomyces albidoflavus* strain TN644 isolated from a Tunisian off-shore oil field, Int. Biodeter. Biodegr. 90 (2014) 36-44. https://doi.org/10.1016/j.ibiod.2014.02.001.

52. S.G. Burton, D.A. Cowan, J.M. Woodley, The search for the ideal biocatalyst, Nat. Biotechnol. 20 (2002) 37-45. https://doi.org/10.1038/nbt0102-37.

53. H. Ogino, H. Ishakawa, Enzymes which are stable in the presence of organic solvents, J. Biosci. Bioeng. 91 (2001) 109-116. https://doi.org/10.1263/jbb.91.109.

54. J. Garcia-Ubasart, T. Vidal, A.L. Torres, O.J. Rojas, Laccase-mediated coupling of nonpolar chains for the hydrophobization of lignocellulose, Biomacromolecules 14 (2013) 1637-1644. https://doi.org/10.1021/bm400291s.

55. E. Ian, D.B. Malko, O.N. Sekurova, H. Bredholt, C. Rückert, M.E. Borisova, A. Albersmeier, J. Kalinowski, M.S. Gelfand, S.B. Zotchev, Genomics of sponge-associated *Streptomyces* spp. closely related to *Streptomyces albus* J1074: Insights into marine adaptation and secondary metabolite biosynthesis potential, PLoS ONE 9 (2014) e96719. https://doi.org/10.1371/journal.pone.0096719.

List of Tables

Table 1: Purification of the DyP-type peroxidase from *Streptomyces albidoflavus* BSII#1.

	Total Protein (mg)	**Total Activity (U*)**	**Specific Activity (U mg^{-1})**	**Yield (%)**	**Purification Factor**
Crude extract	213.00	212.80	1.00	100.00	1.00
Acid fraction	97.93	192.39	1.96	90.40	1.96
Acetone fraction	71.21	174.15	2.45	81.84	2.45
Ultrafiltration: filtrate	0.01	0.67	46.51	0.30	46.51

*One unit (U) of activity equals the amount of enzyme required for the oxidation of 1 µmol of substrate (2,4-DCP) in 1 min.

Table 2: Substrate range and optimal pH for the oxidation of 'typical' peroxidase substrates (n=3; mean±SD) by the peroxidase produced by *Streptomyces albidoflavus* BSII#1. ND = no activity detected; N/A = not applicable.

Substrate	**Substrate extinction coefficient (mM^{-1} cm^{-1})**	**Activity (U ml^{-1})**	**Optimum pH**
2,4-dichlorophenol	ε_{510} = 21.647	1.01±0.06	8.0
2,6-dimethoxyphenol	ε_{468} = 14.8	1.13±0.07	8.0
3-hydroxyanthranilic acid	ε_{452} = 18	ND	N/A
4-methylcatechol	ε_{400} = 1.433	ND	N/A
4-*tert*-butylcatechol	ε_{475} = 3.3	1.60±0.02	8.0
ABTS	ε_{420} = 36	0.13±0.00	3.0
Caffeic acid	ε_{480} = 1.9	0.44±0.04	8.0
Catechol	ε_{410} = 0.74	1.45±0.14	3.0
Guaiacol	ε_{470} = 26.6	0.02±0.00	3.0
L-DOPA	ε_{475} = 3.6	0.62±0.05	8.0
L-tyrosine	ε_{475} = 3.6	ND	N/A
o-aminophenol	ε_{433} = 9.6	1.54±0.11	8.0
p-cresol	ε_{400} = 1.433	ND	N/A
Phenol	ε_{510} = 7.1	1.21±0.04	8.0
Pyrogallol	ε_{450} = 4.4	0.76±0.05	8.0
Resorcinol	ε_{500} = 32.8	ND	N/A
Syringaldazine	ε_{530} = 65	ND	N/A

Table 3: Effect of inhibitors on the partially purified peroxidase from *Streptomyces albidoflavus* BSII#1.

Inhibitor	**Lowest inhibitor concentration resulting in significant inhibition (% inhibition)**	**Complete inhibition at:**
H_2O_2	0.01 mM (42.0%)	0.05 mM
L-cysteine	0.02 mM (33.9%)	0.1 mM
Sodium ascorbate	0.05 mM (39.5%)	0.5 mM
Sodium metabisulphite	0.5 mM (93.5%)	1.0 mM
p-arbutin	1 mM (24.2 %)	Max (66.4%) at 50 mM
Sodium azide	5 mM (26.6%)	Max (68.4%) at 50 mM
EDTA	No inhibition	No inhibition at 50 mM
SDS	No inhibition	No inhibition at 50 mM
NaCl	No inhibition	No inhibition at 50 mM

List of Figures

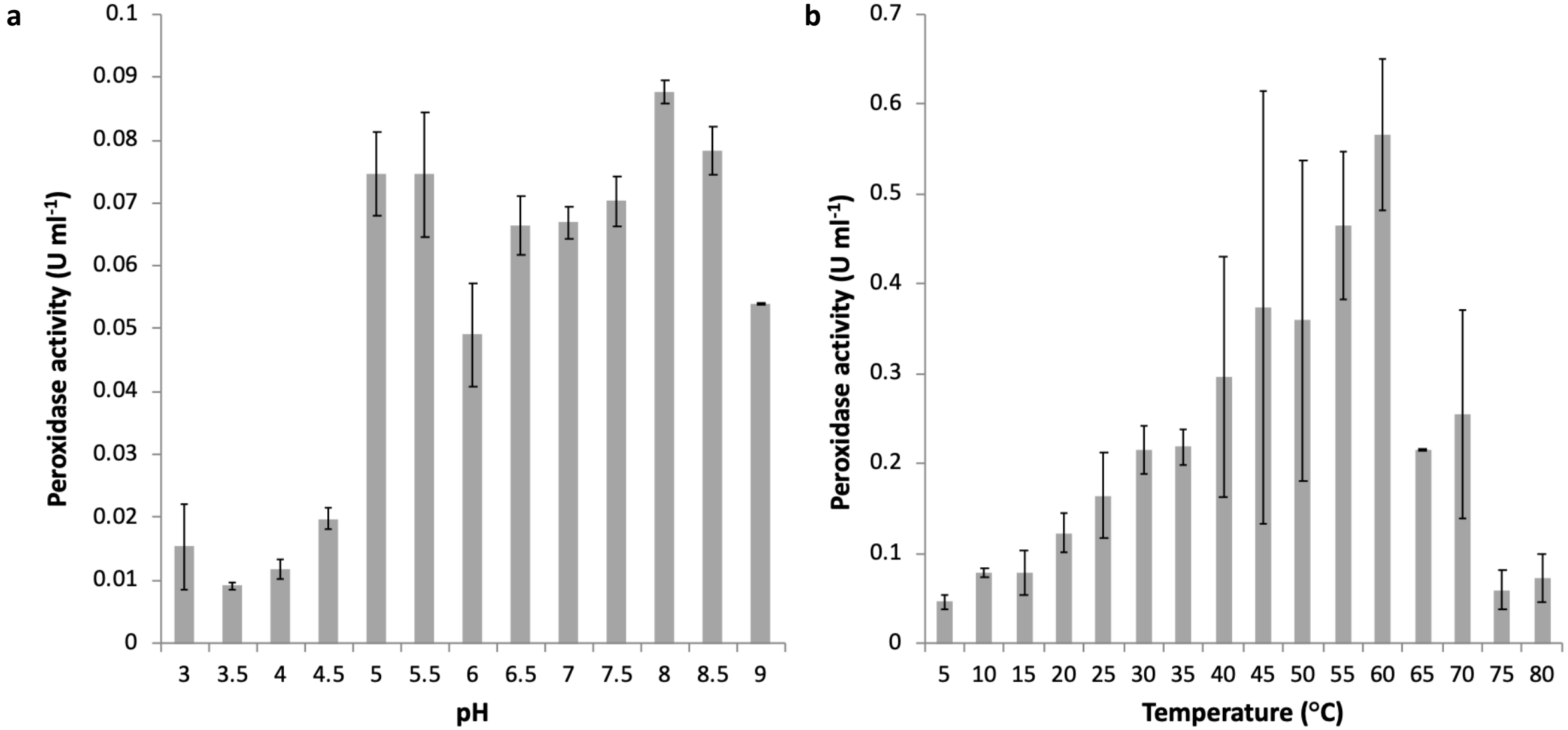
a
Peroxidase activity (U ml-1)
0.1
0.09
0.08
0.07
0.06
0.05
0.04
0.03
0.02
0.01
0
3
3.5
4
4.5
5
5.5
6
6.5
7
7.5
8
8.5
9
pH
b
Peroxidase activity (U ml-1)
0.7
0.6
0.5
0.4
0.3
0.2
0.1
0
5
10
15
20
25
30
35
40
45
50
55
60
65
70
75
80
Temperature (°C)

Figure 1

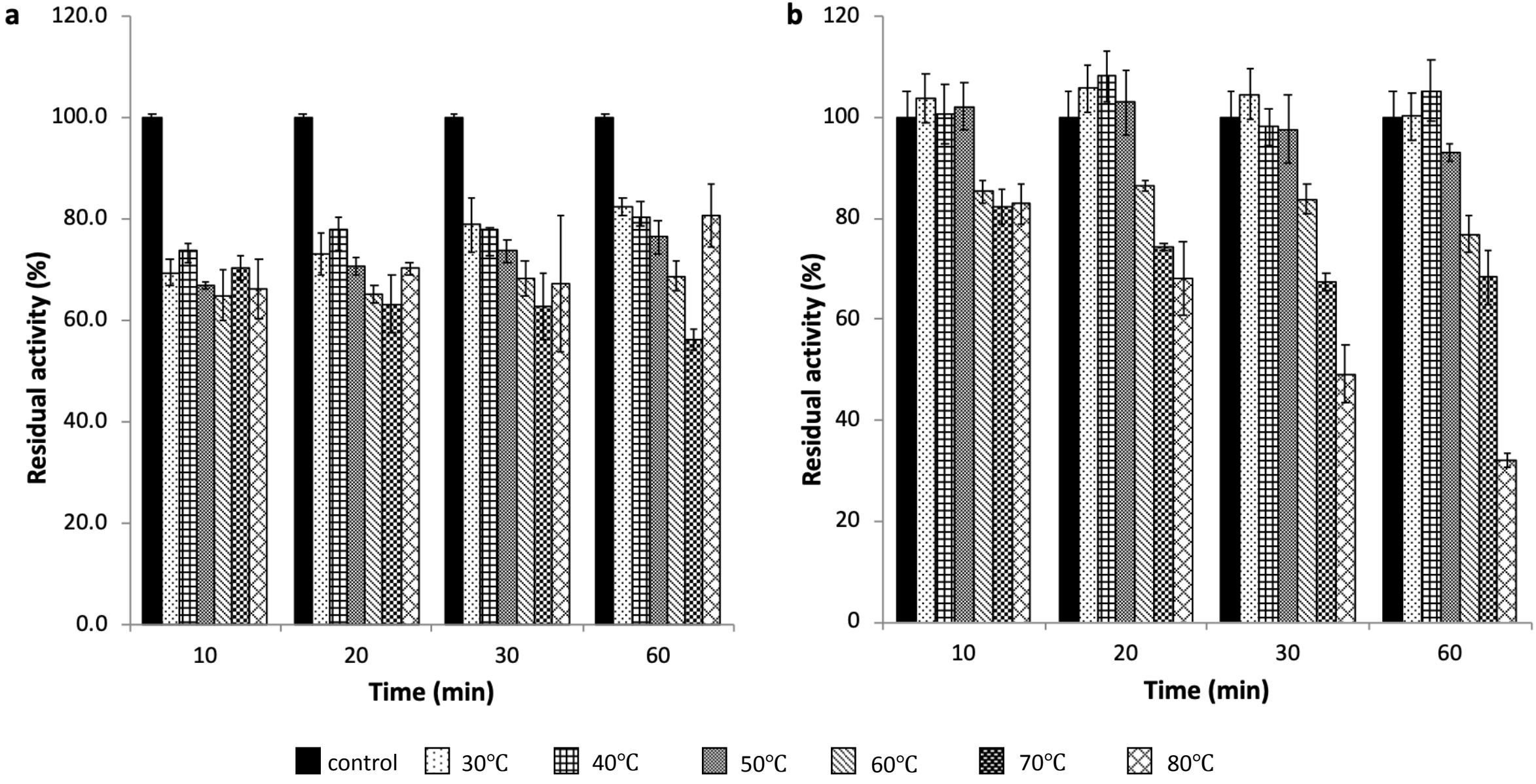
a
120.0
100.0
80.0
60.0
40.0
20.0
0.0
Residual activity (%)
10
20
30
60
Time (min)
b
120
100
80
60
40
20
0
Residual activity (%)
10
20
30
60
Time (min)
control
30°C
40°C
50°C
60°C
70°C
80°C

Figure 2

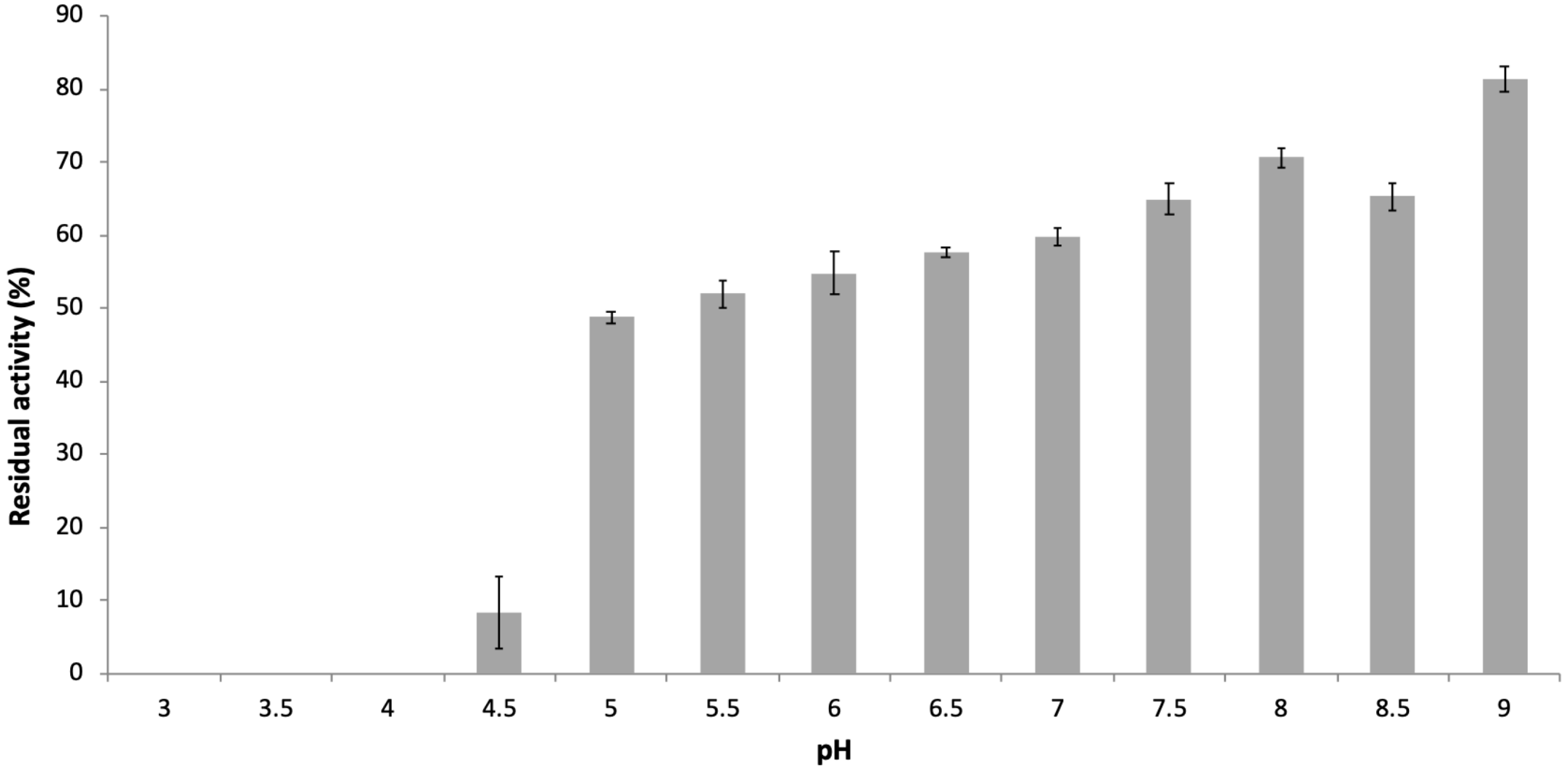
Residual activity (%)
90
80
70
60
50
40
30
20
10
0
3
3.5
4
4.5
5
5.5
6
6.5
7
7.5
8
8.5
9
pH

Figure 3

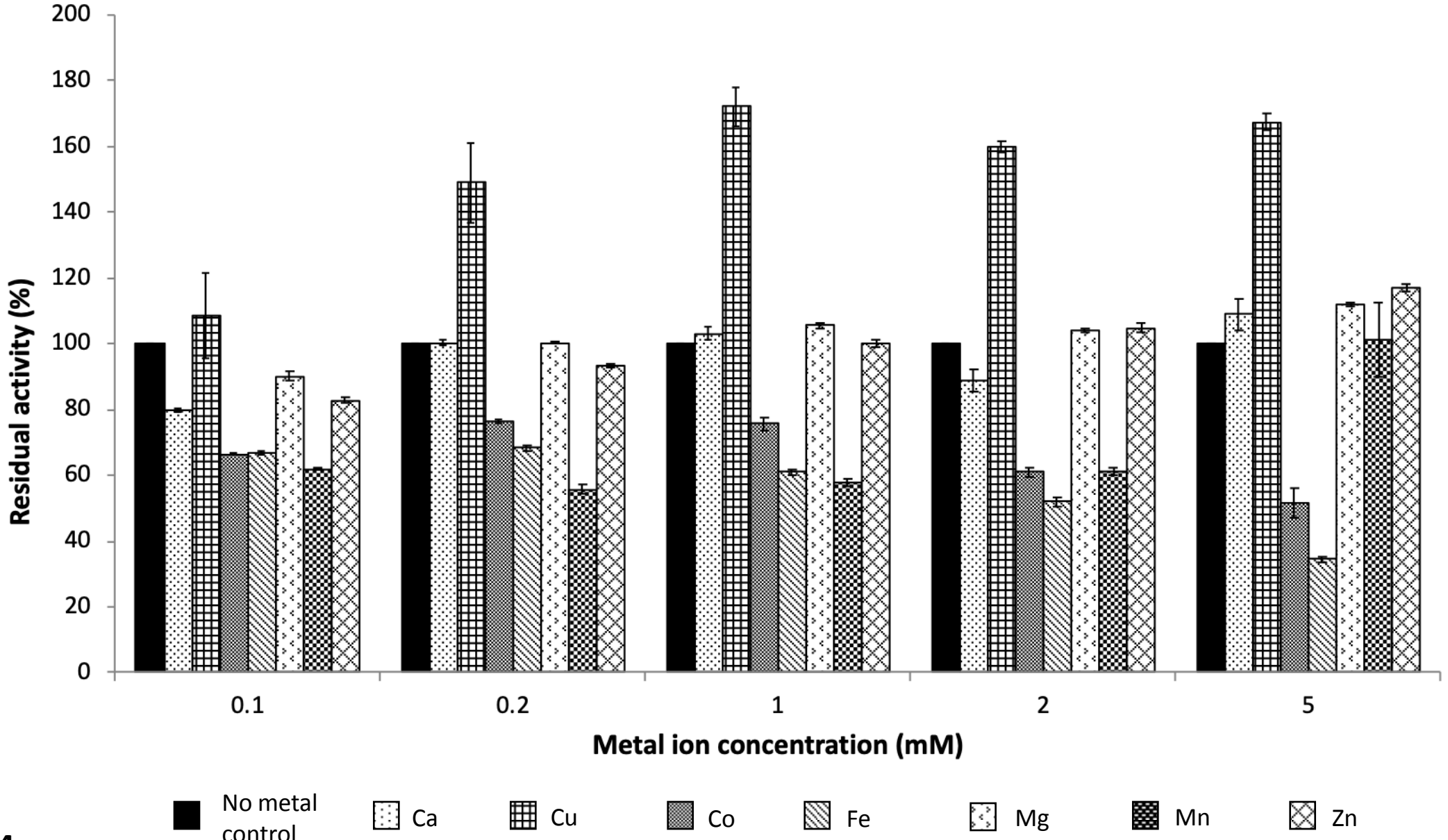
200
180
160
140
120
100
80
60
40
20
0
Residual activity (%)
0.1
0.2
1
2
5
Metal ion concentration (mM)
No metal control
Ca
Cu
Co
Fe
Mg
Mn
Zn

Figure 4

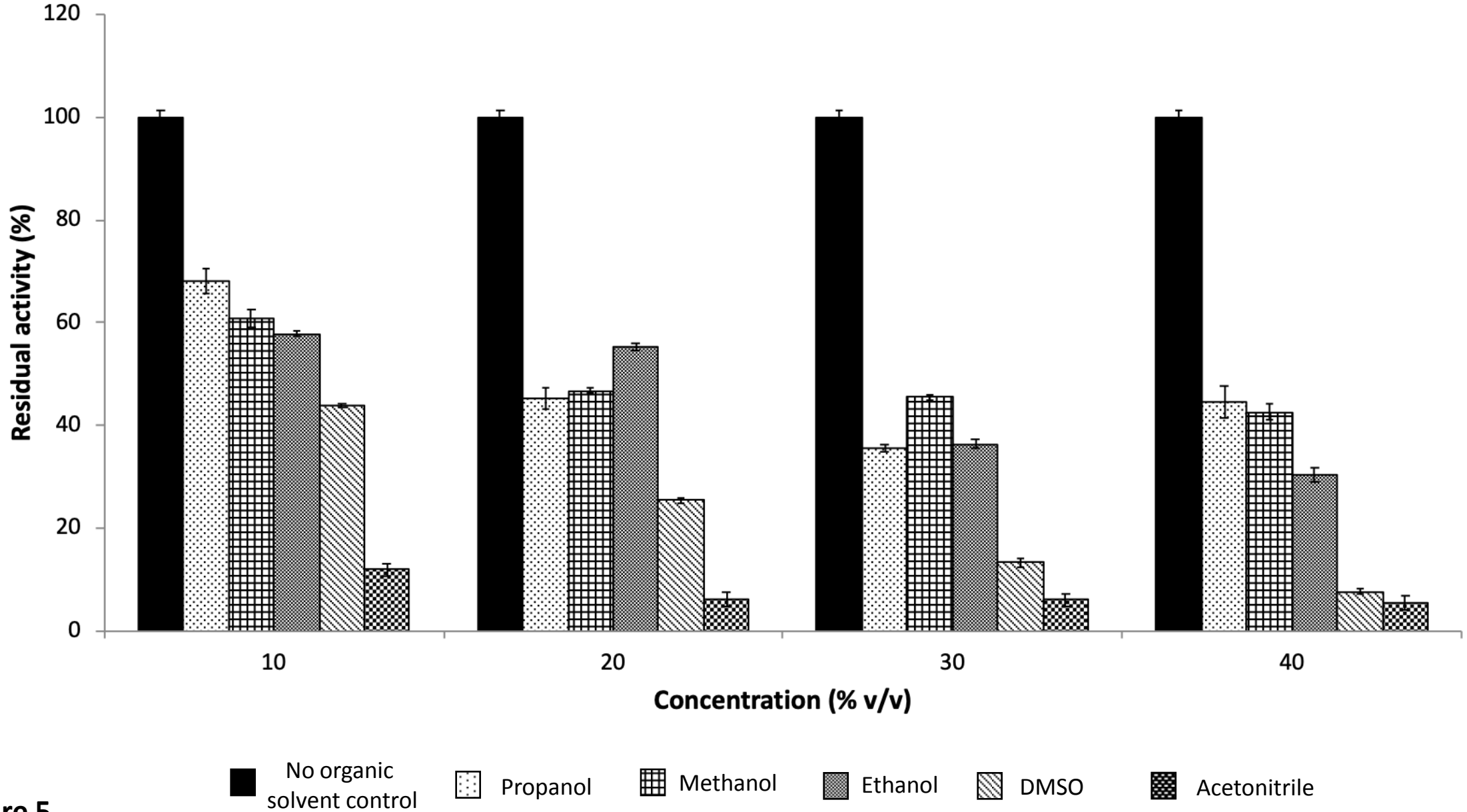
120
100
80
60
40
20
0
Residual activity (%)
10
20
30
40
Concentration (% v/v)
No organic solvent control
Propanol
Methanol
Ethanol
DMSO
Acetonitrile

Figure 5

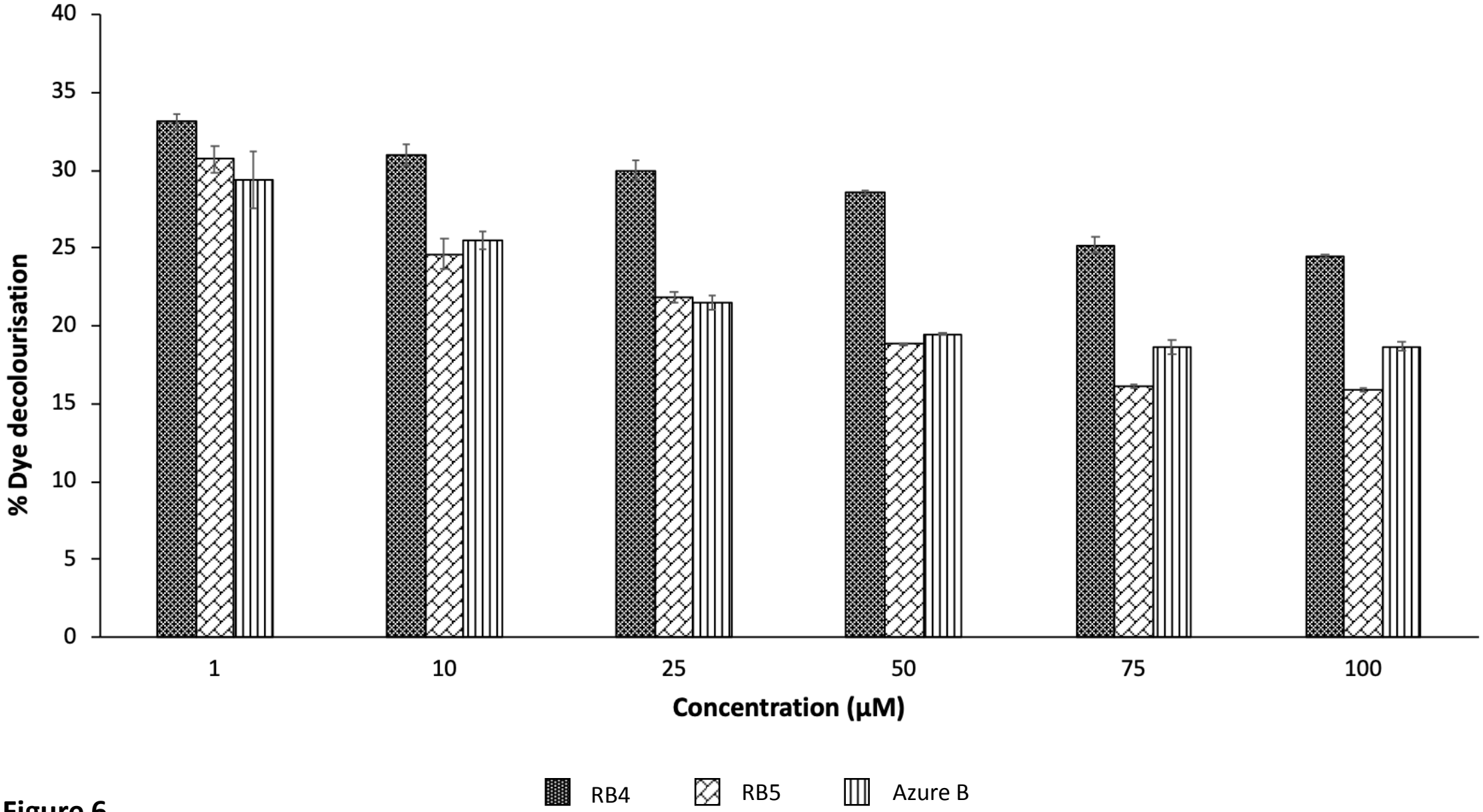
40
35
30
25
20
15
10
5
0
% Dye decolourisation
1
10
25
50
75
100
Concentration (µM)
RB4
RB5
Azure B

Figure 6

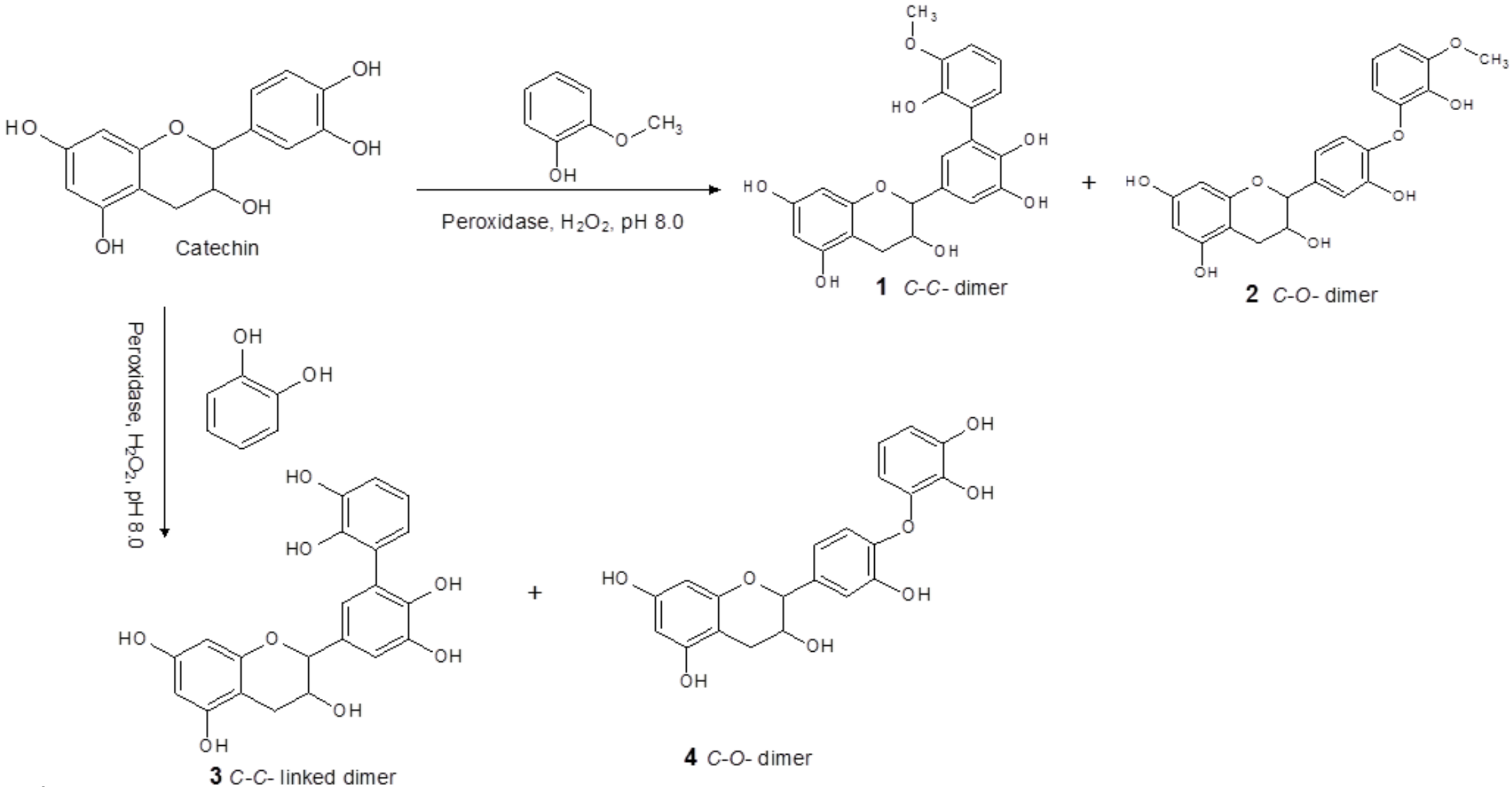
Catechin
Peroxidase, H_2O_2, pH 8.0
1 C-C- dimer
2 C-O- dimer
Peroxidase, H_2O_2, pH 8.0
3 C-C- linked dimer
4 C-O- dimer

Figure 7